Evaluation by Site-Directed Mutagenesis of Aspartic Acid Residues in the Metal Site of Pig Heart NADP-Dependent Isocitrate Dehydrogenase†

Neil B. Grodsky, Sambanthamurthy Soundar, and Roberta F. Colman*

Department of Chemistry and Biochemistry, University of Delaware, Newark, Delaware 19716

Received August 23, 1999; Revised Manuscript Received November 11, 1999

ABSTRACT: Pig heart NADP-dependent isocitrate dehydrogenase requires a divalent metal cation for catalysis. On the basis of affinity cleavage studies [Soundar and Colman (1993) *J. Biol. Chem. 268*, 5267] and analysis of the crystal structure of *E. coli* NADP−isocitrate dehydrogenase [Hurley et al. (1991) *Biochemistry 30*, 8671], the residues Asp^{253}, Asp^{273}, Asp^{275}, and Asp^{279} were selected as potential ligands of the divalent metal cation in the pig heart enzyme. Using a megaprimer PCR method, the Asp at each of these positions was mutated to Asn. The wild-type and mutant enzymes were expressed in *Escherichia coli* and purified. D253N has a specific activity, K_m values for Mn^{2+}, isocitrate, and NADP, and also a pH−V_{max} profile similar to those of the wild-type enzyme. Thus, Asp^{253} is not involved in enzyme function. D273N has an increased K_m for Mn^{2+} and isocitrate with a specific activity 5% that of wild type. The D273N mutation also prevents the oxidative metal cleavage seen with Fe^{2+} alone in the wild-type enzyme. As compared to wild type, D275N has greatly increased K_m values for Mn^{2+} and isocitrate, with a specific activity <0.1% that of wild type, and a large increase in pK_a for the enzyme−substrate complex. D279N has only small increases in K_m for Mn^{2+} and isocitrate, but a specific activity <0.1% that of wild type and a major change in the shape of its pH−V_{max} profile. These results suggest that Asp^{273} and Asp^{275} contribute to metal binding, whereas Asp^{279}, as well as Asp^{275}, is critical for catalysis. Asp^{279} may function as the catalytic base. Using the Modeler program of Insight II, a structure for porcine NADP−isocitrate dehydrogenase was built based on the X-ray coordinates of the *E. coli* enzyme, allowing visualization of the metal−isocitrate site.

NADP-dependent isocitrate dehydrogenase (EC 1.1.1.42) from pig heart catalyzes the oxidative decarboxylation of isocitrate to α-ketoglutarate. The enzyme is known to exist as a homodimer with a subunit molecular mass of 46 600 Da and 413 amino acids (*1*−*3*). NADP-dependent isocitrate dehydrogenase requires a divalent metal ion for enzyme activity (*4, 5*). Several metal ions can be used by the enzyme, including Mn^{2+}, Fe^{2+}, Cd^{2+}, Zn^{2+}, Co^{2+}, or Mg^{2+} (*6*−*8*), with the highest activity being obtained with Mn^{2+} (*6*). Direct binding experiments indicate that NADP-dependent isocitrate dehydrogenase binds 1 mol of Mn^{2+}/mol of enzyme subunits (*5*). It is thought that the metal−isocitrate complex is the preferred substrate for this enzyme (*4*), and essentially the same dissociation constant for Mn^{2+}-isocitrate from the enzyme can be calculated from direct binding measurements of Mn^{2+} in the presence of isocitrate and from kinetic determinations of K_m (*5, 6, 9*). Kinetics, binding, and affinity cleavage experiments suggest that the metal ion occupies different sites in the absence and presence of isocitrate, the substrate (*4, 9, 10*).

Although there is not yet a crystal structure of any mammalian NADP-dependent isocitrate dehydrogenase, the structure of the *Escherichia coli* enzyme has been solved (*11*−*13*). In the Mg^{2+}-isocitrate complex of the *E. coli* enzyme, the Mg^{2+} is coordinated by Asp^{307}, while Asp^{311} is a second nearest neighbor to the metal ion (*12*). Alignment of the amino acid sequences of the porcine and *E. coli* enzymes indicates that only 14% identity (plus about 34% similarity) exists between the mammalian and *E. coli* enzymes. However, the regions of the amino acid sequences that interact with isocitrate and the divalent metal ion appear to contain some conserved amino acid residues (*3, 11*−*13*). For example, as shown in Figure 1, the porcine enzyme's Asp^{275} and Asp^{279} can be aligned, respectively, with Asp^{307} and Asp^{311} of the *E. coli* enzyme.

Affinity cleavage studies on porcine NADP-dependent isocitrate dehydrogenase (*10*) have shown that, in the presence of O_2, Fe^{2+} produces oxidative cleavage between Tyr^{272} and Asp^{273}, suggesting Asp^{273} as a coordination site for Fe^{2+} and, by implication, Mn^{2+}. Fe^{2+}-isocitrate produces mutually exclusive cleavages between Asp^{253}−Met^{254} or His^{309}−Gly^{310}, suggesting Asp^{253} and/or His^{309} as coordination sites for Fe^{2+}-isocitrate and, by implication, Mn^{2+}-isocitrate.

It has been previously shown that the pH dependence of V_{max} for porcine NADP-dependent isocitrate dehydrogenase yields a pK of about 5.7 (*14*). This pK is independent of temperatures from 10 to 30 °C (*14*) and increases to about 6.3 in 20% ethanol (*15*). These results imply that this pK represents ionization of a carboxyl group in the enzyme−substrate complex, rather than another type of side chain such as a cationic acid (*16*−*18*), which suggests that a carboxyl

† This work was supported by U.S. Public Health Service Grant DK39075.

* To whom correspondence should be addressed. Phone: 302-831-2973. FAX: 302-831-6335. E-mail: rfcolman@Udel.edu.

10.1021/bi9919753 CCC: $19.00
Published on Web 02/08/2000

Porcine	^{250}LIDD^{253}MVA-----QVLKSSGGF-VWACKNYD^{273}GD^{275}VQSD^{279}ILA^{282}
Rat	^{250}LIDD MVA-----QAMKSEGGF-IWACKNYD GD VQSD SVA^{282}
Yeast	^{251}LIDD MVA-----QMIKSKGGF-IMALKNYD GD VQSD IVA^{283}
E. coli	^{276}VIKD VIADAFLQQILLRPAEYDVIACMNLN GD YISD ALA^{314}

FIGURE 1: Amino acid sequence alignment of a selected region of NADP-dependent isocitrate dehydrogenases from porcine heart mitochondria (Porcine), rat cytoplasm (Rat), yeast mitochondria (Yeast), and *E. coli*. The alignment was done with CLUSTAL W. The boldface Asp residues were mutated to Asn for this study.

group is involved in catalysis.

Based on the sequence alignment of the mammalian and *E. coli* enzymes (Figure 1) and comparison with the *E. coli* enzyme's crystal structure, as well as the affinity cleavage studies, Asp^{253}, Asp^{273}, Asp^{275}, and Asp^{279} have been postulated to contribute to metal binding. To identify amino acid residues important for metal binding to pig heart NADP-dependent isocitrate dehydrogenase, Asp^{253}, Asp^{273}, Asp^{275}, and Asp^{279} were mutated to Asn. In this paper, we report that Asp^{273} is important for binding metal ion in the absence of isocitrate, whereas Asp^{275} contributes to the binding of metal ion in the presence of isocitrate, as well as to some other catalytic function. Asp^{279} also appears to have an important role in catalysis. A preliminary version of this study has been presented (*19*).

EXPERIMENTAL PROCEDURES

Materials. Chemicals, biochemicals, and buffer components were purchased from Sigma Chemical Co. (St. Louis, MO) unless otherwise noted. Human plasma thrombin was obtained from Enzyme Research Laboratories (South Bend, IN). EDTA[1] (disodium salt), ferrous sulfate, sodium sulfate (anhydrous), and manganous sulfate were from Fisher Scientific. Acrylamide, bisacrylamide, and glycine were purchased from BioRad (Hercules, CA). Restriction enzymes were purchased from Life Technologies. T4 DNA ligase, pMAL-c2, *E. coli* strain TB1, amylose resin, and Vent polymerase were from New England Biolabs (Beverly, MA). Cloned Pfu polymerase was obtained from Stratagene (La Jolla, CA). Calf intestinal alkaline phosphatase was from Promega Corp. (Madison, WI). Matrex Gel Red A, Amicon centricons, and CM membranes were from Millipore Corp. (Bedford, MA). Low molecular weight standards were purchased from Amersham Pharmacia Biotech (Piscataway, NJ). Oligonucleotides were synthesized by Operon Technologies (Alameda, CA). Sequencing primers were synthesized by LI-COR (Lincoln, NE).

Vector Construction. The 1.2 kbp cDNA encoding pig heart NADP-dependent isocitrate dehydrogenase (IDP1) was cloned into vector pMAL-c2 (pMALcIDP1) as previously described (*20*). In addition to the *Bam*HI restriction site at the C-terminus of IDP1, there is a Bpu1102 I restriction site in MalE, 0.4 kbp from the N-terminus of IDP1. The recombinant mammalian enzyme is expressed as a maltose binding fusion protein to facilitate purification from the *E. coli* isocitrate dehydrogenase.

Site-Directed Mutagenesis. Site-directed mutagenesis of pMALcIDP1 was performed using a PCR megaprimer method (*21, 22*). For the first PCR reaction, a total volume of 50 μL containing 500 ng each of the mutagenic primer and the *Bam*H IR universal reverse primer, 100 ng of 7.8 kbp template, 2.5 units of cloned Pfu polymerase, and 5.0 μL of 10 $\times$ Pfu polymerase buffer was used to amplify a DNA fragment stretching from the region being mutated to the end of IDP1, the *Bam*HI site. PCR reactions were performed on a Robocycler Gradient 96 (Stratagene) with a heated lid in place. Following an initial denaturation step (95 °C for 1 min), 30 PCR cycles were carried out, each consisting of 95 °C for 1 min, 55 °C for 1 min, and 72 °C for 2.5 min. A final extension step (72 °C for 10 min) was performed. This DNA fragment, known as the megaprimer, was purified and recovered by agarose gel electrophoresis and the Ultraclean 15 DNA Purification kit (MoBio Laboratories, Solana Beach, CA). For the second PCR reaction, a total volume of 50 μL containing 500 ng each of the megaprimer and the BpuF universal foward primer, 100 ng of 7.8 kbp template, 2.5 units of cloned Pfu polymerase (2.0 units of Vent polymerase for the D253N mutant), and 5.0 μL of 10 $\times$ Pfu polymerase buffer was used to amplify a 1.6 kbp DNA fragment which includes IDP1 (1.2 kbp; the enzyme) and a small portion of MalE (the maltose binding protein). The same PCR program was used in this reaction as mentioned for the first reaction. This PCR product was treated with 0.2% SDS and proteinase K (2 μg/50 μL of reaction) for 30 min at 55 °C to denature and digest the Pfu polymerase. The DNA was purified by phenol/chloroform extraction and concentrated by ethanol precipitation. To remove the overhangs, the 1.6 kbp DNA fragment was digested with *Bam*HI and Bpu1102 I (20 units of each) for 5 h, followed by purification and recovery by agarose gel electrophoresis and the Ultraclean 15 DNA Purification Kit. The 1.6 kbp PCR product was ligated to the remaining 6.3 kbp of pMAL-c2 (which had previously been treated with 1 unit of calf intestinal alkaline phosphatase to dephosphorylate the 5′ end) by the following procedure: 0.22 pmol of 1.6 kbp insert was added to 0.075 pmol (0.3 μg) of 6.3 kbp vector and water and incubated at 55 °C for 10 min to denature any cohesive termini that have reannealed. The solution was chilled to 0 °C, followed by addition of 1 μL of 10 $\times$ ligase buffer (ATP included) and 1 μL of T4 DNA ligase. The reaction was incubated for 16 h at 16 °C, followed by transformation with competent *E. coli* strain TB1 cells. DNA was purified using the Wizard Plus Maxiprep DNA Purification Kit (Promega Corp.). Ligations were evaluated by restriction digestion with *Bam*HI and Bpu1102 I, followed by agarose gel electrophoresis. The oligonucleotides that were used to introduce the D253N, D273N, D275N, and D279N substitutions (underlined) were, respectively, 5′-CACCGGCTCATTGAT<u>AAC</u>ATGGTGCTCAG-3′, 5′-CCTGCAAGAAC TAC<u>AAT</u>GGAGACGTGC-3′, 5′-GAACTACGATGGA<u>AAC</u>GTGCAGTCGGAC-3′, and 5′-GAGACGTGCA-GTC<u>GAAC</u>ATCCTGGCCC-3′. The universal primers *Bam*H IR and BpuF were, respectively, 5′-CTA-

[1] Abbreviations: EDTA, ethylenediaminetetraacetic acid; PCR, polymerase chain reaction; IPTG, isopropyl thio-β-D-galactopyranoside; CD, circular dichroism; FPLC, fast-performance liquid chromatography; SDS, sodium dodecyl sulfate.

GAGGATCCTTACTACTGCCGGCCCAGAGCTCTGTC-3′ and 5′-GGCGTGCTGAGCGCAGGTATTAACGCCGC-CAGTCCG-3′. All mutations were confirmed by nucleotide sequence analysis via the dye primer cycle sequencing method using a LI-COR 4200 Long Readir Sequencer at the University of Delaware's Cell Biology Core Facility.

The plasmids were expressed in *E. coli* strain TB1, and the recombinant wild-type and mutant isocitrate dehydrogenases were purified to homogeneity as previously described (*20*) except that the enzyme was expressed for 24 h at 25 °C after IPTG induction, thrombin cleavage was allowed to proceed for 48 h, and the Superose-12 FPLC column for the final purification step was omitted. Since the porcine isocitrate dehydrogenase is expressed as a fusion protein with maltose binding protein, it binds tightly to the amylose resin column while the intrinsic *E. coli* enzyme is completely washed off, as detected by the sensitive enzymatic activity assay, as well as by protein determination (*20*). This separates entirely the mammalian isocitrate dehyrogenase from the bacterial enzyme. Thrombin cleavage of the fusion protein is carried out after the amylose column. The purity of the mutant proteins was assessed by 15% SDS−polyacrylamide gel electrophoresis (*23*) and N-terminal amino acid sequencing on an Applied Biosystems gas-phase sequenator (model 470A) equipped with an on-line phenylthiohydantoin analyzer (model 120) and a computer (model 900A). The enzyme was stored at −80 °C in 0.1 M triethanolamine chloride (pH 7.7) containing 10% glycerol and 0.3 M Na_2SO_4.

Circular Dichroism of the Wild-Type and Mutant Enzymes. CD was conducted using a Jasco model J-710 spectropolarimeter. Measurements of the ellipticity as a function of wavelength at 0.1 nm increments between 250 and 200 nm were made using a 0.1 cm path length cylindrical quartz cell. Purified protein samples (0.15 mg/mL) were prepared in 25 mM triethanolamine chloride (pH 7.7) containing 10% glycerol and 75 mM Na_2SO_4. Each scan was repeated 5 times and averaged. Background from the buffer was subtracted from all spectra. The mean molar ellipticity, $[\theta]$ (deg cm^2 dmol^{-1}), was calculated from $[\theta] = \theta/10nCl$, where θ is the measured ellipticity (millidegrees), C is the molar concentration of protein (molar), l is the cell path length (centimeters), and n is the number of residues per subunit of enzyme (413 for NADP-dependent isocitrate dehydrogenase).

FPLC of the Wild Type and Mutants. Gel filtration was conducted using a Superose-12 column (1 × 30 cm; Pharmacia), equilibrated with 0.1 M triethanolamine chloride (pH 7.7) containing 10% glycerol and 0.3 M Na_2SO_4, connected to a Pharmacia FPLC system. For each sample, 0.35 mL of 0.9 mg/mL purified protein was applied to the column at a flow rate of 0.3 mL/min. Molecular weight calibration kits containing Blue Dextran 2000, catalase (232 kDa), aldolase (158 kDa), albumin (67 kDa), ovalbumin (43 kDa), and chymotrypsinogen (25 kDa) (Amersham Pharmacia Biotech) were used to generate a standard curve.

Kinetics of Wild-Type and Mutant NADP-Dependent Isocitrate Dehydrogenases. Enzyme assays were performed at 25 °C by monitoring the time-dependent reduction of NADP to NADPH at 340 nm. The assay solution (1 mL) contained 30 mM triethanolamine chloride (pH 7.4), 0.1 mM NADP, 4 mM DL-isocitrate, and 2 mM $MnSO_4$, unless otherwise noted. One unit of enzyme activity is defined as the amount of enzyme that catalyzes the reduction of 1 μmol of NADP/min under the assay conditions. The specific activity is defined as the number of enzyme units per milligram of protein. The protein concentration for purified enzyme was determined from $E^{1\%}_{280nm} = 10.8$ (*24*). A subunit molecular mass of 46 600 Da (*3*) was used to calculate the concentration of enzyme subunits.

For K_m determinations, the concentration of either isocitrate, Mn^{2+}, or NADP was varied, and the other substrates were maintained at the standard, saturating conditions. The K_m values were determined from Lineweaver−Burk plots, and error measurements were determined from Sigma Plot.

The pH−rate profiles for the reaction catalyzed by the wild type and mutants were determined over the range of pH 5−8. The buffers contained 30 mM sodium acetate (pH 5.0−6.0), 30 mM imidazole chloride (pH 6.0−7.6), or 30 mM triethanolamine chloride (pH 6.9−8.0). (All of the buffers are 30 mM in anion concentration.) The reaction rate was measured using 0.1 mM NADP, 4 mM isocitrate, and 2 mM $MnSO_4$, unless indicated otherwise.

Inactivation and Affinity Cleavage of Porcine NADP-Dependent Isocitrate Dehydrogenase by Fe^{2+} or Fe^{2+} and Isocitrate. Wild type, D253N, and D273N (11 μM) were incubated with 20 mM ascorbate, with or without the addition of 20 μM ferrous sulfate (wild type, D273N), or with or without the addition of 20 μM ferrous sulfate and 4 mM isocitrate (wild type, D253N) in 0.1 M triethanolamine chloride (pH 7.7) containing 10% glycerol and 0.3 M Na_2SO_4 at 25 °C for 3 h, as was previously described for the porcine heart enzyme (*10*). EDTA (4 mM) was added directly to the incubation mixture in order to quench the inactivation of the enzyme caused by Fe^{2+}. Aliquots from the reaction mixture were assayed for residual enzyme activity after 3 h. Aliquots were screened by SDS−polyacrylamide gel electrophoresis to detect the presence of fragments generated by cleavage of the enzyme.

Molecular Modeling of Porcine NADP-Dependent Isocitrate Dehydrogenase. Since the crystal structure of porcine NADP-dependent isocitrate dehydrogenase has not yet been solved, modeling studies were carried out on an SGI workstation using Insight II (Biosym/MSI, San Diego, CA). The structure of NADP-dependent isocitrate dehydrogenase from *E. coli* (*12*) was used as a reference model. The alignment of the sequences from porcine heart, *E. coli*, yeast mitochondria, and rat cytoplasm was obtained using CLUSTAL W.

The modeling was performed using the Modeler program under Homology. This is an automated homology modeling program that calculates an all-atom model using combined information from the sequence alignment and the structure of the reference protein. Spatial restraints, expressed as probability density functions (PDFs) from the reference protein, are optimized to obtain the model. The model with the lowest value of objective function (F, molecular PDF violation) fits best to the reference structure. In the search

[2] For example, amino acids 1, 5, and 8 are, respectively, Ala, Ile, and Ala for the porcine enzyme, with Met, Val, and Pro for the *E. coli* enzyme. The results of N-terminal sequencing yielded the following data: amino acid 1 (351.3 pmol of Ala, 0.8 pmol of Met); amino acid 5 (115.6 pmol of Ile, 0 pmol of Val); and amino acid 8 (133.2 pmol of Ala; 0 pmol of Pro).

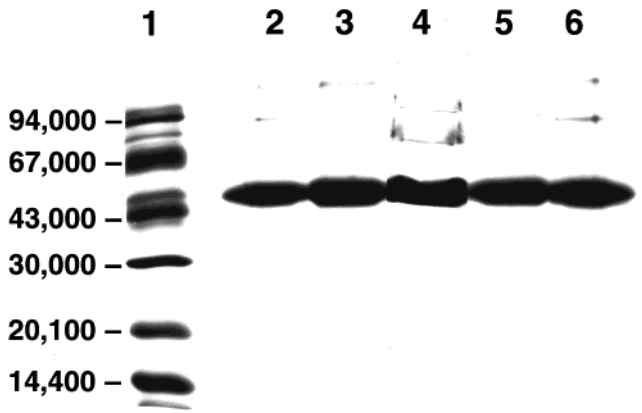

FIGURE 2: SDS−PAGE of purified wild-type and mutant enzymes. Wild type (lane 2), D253N (lane 3), D273N (lane 4), D275N (lane 5), and D279N (lane 6). Lane 1 contains protein standards.

for the best alignment, three models were generated from each different alignment using the medium optimization protocol (fast molecular dynamics simulated annealing). The best alignment was selected by comparing the lowest *F* values. To simplify the procedure, a monomer was analyzed.

RESULTS

Protein Purity. The purity of the recombinant porcine NADP-dependent isocitrate dehydrogenase wild type and mutants was assessed by SDS−polyacrylamide gel electrophoresis. As shown in Figure 2, the wild type and mutants were purified to greater than 95% purity. The porcine and *E. coli* enzymes differ in 9 of the first 10 amino acids. N-Terminal amino acid sequencing of the wild-type and mutant porcine enzymes showed they are pure, and are not contaminated with the *E. coli* enzyme.[2]

Circular Dichroism Spectra of Wild-Type and Mutant Enzymes. CD spectra were measured for the mutant and wild-type enzymes to evaluate whether changes in the secondary structure of the enzyme resulted from the mutations at positions 253, 273, 275, or 279. The CD spectra of all the mutants were similar (within experimental error) to that of wild type, with minima occurring at 208 and 223 nm (data not shown). These results indicate that the mutations do not cause appreciable change in the secondary structure of the enzyme.

The % α-helix in the active form of the enzyme can be estimated from the equation (*25*):

$$\%\ \alpha\text{-helix} = \frac{[\theta]_{280\text{nm}} - 4000}{33000 - 4000} \times 100$$

where $[\theta]_{208\text{nm}}$ is the mean residue molar ellipticity at 208 nm. The recombinant wild-type and mutant NADP-dependent isocitrate dehydrogenases were estimated to have an α-helical content of about 28%. This is in agreement with the previously calculated % α-helix value for the pig heart enzyme of 27% (*26*).

Gel Filtration FPLC of the Wild-Type and Mutant Enzymes. To assess whether the recombinant porcine NADP-dependent isocitrate dehydrogenase is a dimer, and whether any of the mutations influenced the oligomeric state of the enzyme, gel filtration was conducted under native conditions (in 0.1 M triethanolamine chloride, pH 7.7, containing 10% glycerol and 0.3 M Na_2SO_4). Wild-type recombinant NADP-dependent isocitrate dehydrogenase elutes between aldolase (158 kDa) and albumin (67 kDa) (data not shown). The data are consistent with a protein of about 93 kDa, the dimeric form of the enzyme. No absorbance is observed in the region of monomer elution.

Table 1: Kinetic Parameters for Wild-Type and Mutant NADP-Dependent Isocitrate Dehydrogenases: Specific Activity and K_m for Mn^{2+}

enzyme	sp act.[a] (μmol min^{-1} mg^{-1})	$K_m(Mn^{2+})$[b] (μM)	$k_{cat}/K_m \times 10^{-6}$ ($s^{-1}\,M^{-1}$)
wild type	41	1.1 ± 0.16	28
D253N	33	0.56 ± 0.044	44
D273N	2.0	63 ± 7.3	0.025
D275N	0.039	240 ± 19	0.00013
D279N	0.030	nd[c]	nd[c]

[a] The specific activities were measured in 30 mM triethanolamine chloride (pH 7.4) under standard assay conditions described under Experimental Procedures. [b] The K_m and k_{cat} values were determined by varying the concentration of Mn^{2+} and maintaining the concentrations of the other substrates at the standard saturating conditions. The data were analyzed by Michaelis−Menten and Lineweaver−Burk plots. [c] The K_m for Mn^{2+} for the D279N mutant could not be determined accurately at pH 7.4 because the enzyme activity is low and, with the relatively high concentrations of enzyme required, the endogenous metal ion interfered with the assays. Instead, this K_m value was determined from activity measurements in 0.2 M sodium acetate (pH 5.0) in the presence of 0.1 mM NADP and 4 mM isocitrate, as indicated in the text.

The same experiments were carried out on all of the mutants. All of the mutant enzymes were eluted at close to the same position as wild type (data not shown). The results suggest that the mutations do not affect the oligomeric state of the enzyme.

Kinetic Parameters of the Wild-Type and Mutant Enzymes. To evaluate the metal site of porcine NADP-dependent isocitrate dehydrogenase, Asp was mutated to Asn at positions 253, 273, 275, and 279. The kinetic parameters of these mutants are summarized in Tables 1 and 2. Table 1 shows that the specific activities of the D275N and D279N mutants are <0.1% that of wild type, while the D273N mutant has a specific activity about 5% that of wild type. In contrast, the D253N mutant is similar in specific activity to wild type. Table 1 also illustrates that the D273N and D275N mutants have greatly increased K_m values for Mn^{2+} (60- and 200-fold, respectively) as compared to wild type, whereas the D253N mutant exhibits a K_m value for Mn^{2+} similar to that of wild type. Because the specific activity of the D279N mutant was significantly higher as the pH was decreased, its K_m for Mn^{2+} was measured at pH 5.0, as described in the legend of Table 1. Under these conditions, wild type exhibits a K_m for Mn^{2+} of 43 ± 2.1 μM, and the D253N enzyme has a K_m of 35 ± 2.6 μM, while that of the D279N mutant was 13 ± 0.7 μM. Thus, the K_m for Mn^{2+} of the D279N mutant is also not changed appreciably as compared to wild-type enzyme. The results suggest that Asp^{273} and Asp^{275} contribute to the binding of Mn^{2+} by porcine NADP-dependent isocitrate dehydrogenase.

Table 2 indicates that the D273N mutant exhibits a small increase in K_m for isocitrate, while the D275N mutant has a 25-fold increase in K_m for isocitrate as compared to wild type. The D253N and D279N mutants have K_m values for isocitrate that are similar to that of wild type. Furthermore, all of the mutants studied here have K_m values for the coenzyme, NADP, which are similar to that of wild type.

Table 2: Kinetic Parameters for Wild-Type and Mutant NADP-Dependent Isocitrate Dehydrogenases: K_m for NADP and Isocitrate[a]

enzyme	K_m(NADP) (μM)	$k_{cat}/K_m \times 10^{-6}$ (s^{-1} M^{-1})	K_m(isocitrate) (μM)	$k_{cat}/K_m \times 10^{-6}$ (s^{-1} μM^{-1})
wild type	8.4 ± 0.71	3.7	4.3 ± 0.23	7.2
D253N	9.8 ± 2.1	2.6	2.4 ± 0.20	10
D273N	10 ± 1.3	0.16	12 ± 0.98	0.14
D275N	24 ± 3.3	0.0013	103 ± 13.	0.00030
D279N	10 ± 0.60	0.0028	1.4 ± 0.22	0.020

[a] The K_m constants were determined by varying the concentrations of NADP or isocitrate and maintaining the other substrates at the standard saturating conditions. The data were analyzed by Michaelis−Menten and Lineweaver−Burk plots.

The pH−rate profiles were determined for the wild-type and mutant enzymes to evaluate the effects on the ionizable groups caused by the mutations. Measurements were made using 2 mM Mn^{2+}, 4 mM isocitrate, and 0.1 mM NADP. Figure 3 shows the plots of $V_{max,obs}$ (specific activity) against pH for the wild-type and mutant enzymes. Note that due to the large differences in specific activities, the scales for the *y*-axes are different for the individual graphs. Over the pH range 5−8, the pH−rate profiles for D253N (Figure 3A) and D273N (Figure 3B) are similar to that of wild type (Figure 3A), whereas the pH−rate profile for D275N (Figure 3C) is shifted toward higher pH as compared to wild type. In Figure 3C, $V_{max,obs} - V_{max,lim}$ was plotted against pH because at low pH, $V_{max,obs}$ went to a constant rate, $V_{max,lim}$, of 0.0046 μmol min^{-1} mg^{-1}, instead of 0. Since $V_{max,lim}$ is low (0.01% that of wild type), it may represent a low rate of catalysis when the ionizing group is protonated. In contrast to wild type, the $V_{max,obs}$ for D279N (Figure 3D) actually decreases with increasing pH, suggesting that the rate is higher when a particular ionizable group is protonated. Under the experimental conditions for Figure 3, using double the concentrations of isocitrate, Mn^{2+}, and NADP, the pH−rate profiles for the wild type and mutants were similar to those under standard conditions, indicating that the enzyme is saturated with respect to substrates and that the pH−rate profiles are actually the pH dependence of V_{max}. Representative data for D275N are shown in Figure 3C. The data of Figure 3A,B were analyzed by the equation:

$$V_{max,obs} = V_{max,int}/(1 + [H^+]/K_a)$$

which was analyzed by double-reciprocal plots of $1/V_{max,obs}$ vs $[H^+]$, where $V_{max,obs}$ is the specific activity measured experimentally at every pH, and $V_{max,int}$ is the pH-independent

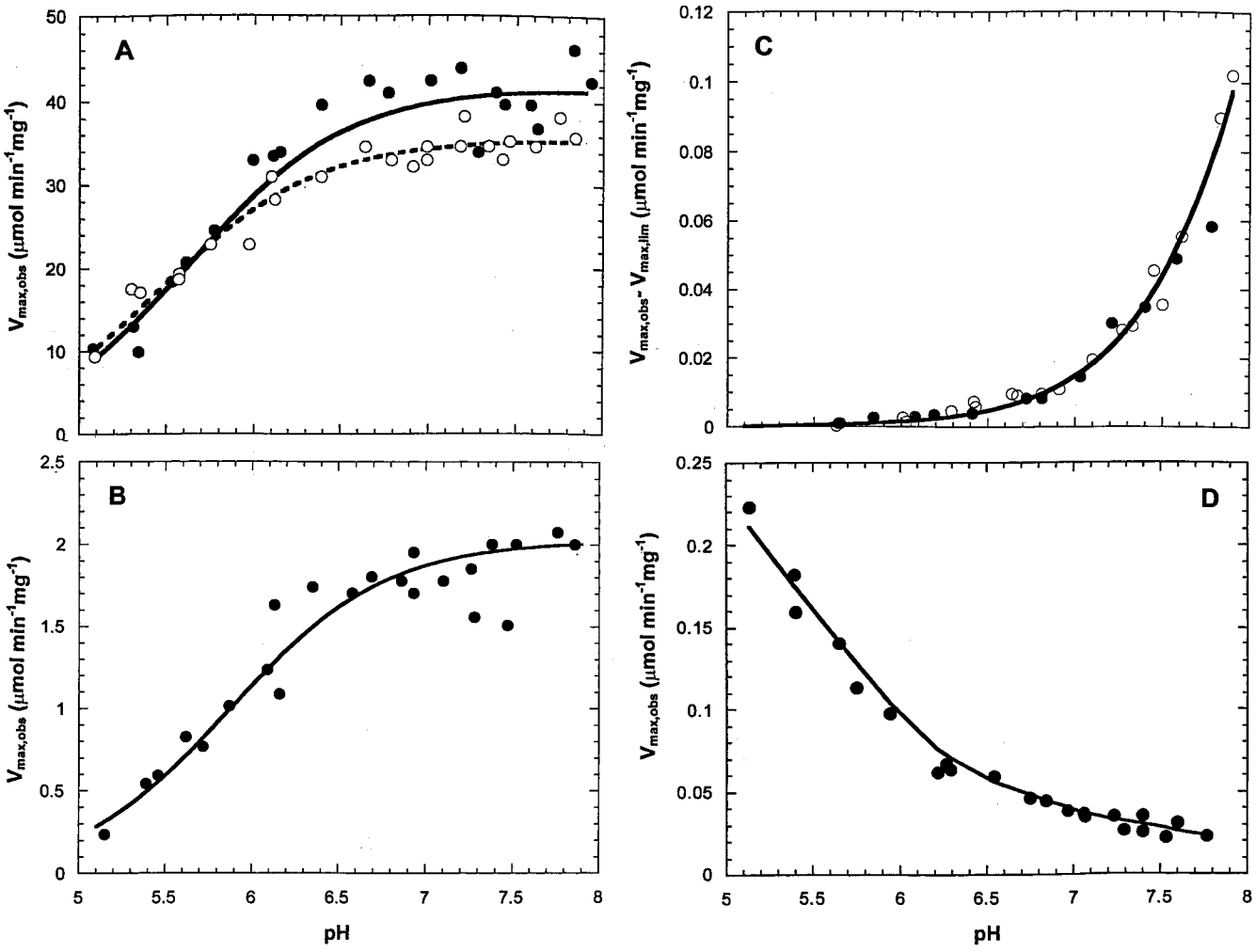

FIGURE 3: pH−rate profiles for the wild-type and mutant enzymes. The activities in different pH buffers were measured for the wild type (A, ●, solid line), D253N (A, ○, dashed line), D273N (B), D275N (C), and D279N (D) enzymes, as described under Experimental Procedures. For D275N (C), the pH−rate profile measured under standard conditions is represented by (●), whereas the pH−rate profile measured using twice the standard concentration of substrate and cofactor is represented by (○). Please note that due to the differences in specific activities, the scales for the *y*-axes are different on graphs (A)−(D).

Table 3: Kinetic Parameters for the pH−Rate Profiles for Wild-Type and Mutant NADP-Dependent Isocitrate Dehydrogenases

enzyme	pK_{es}	$V_{max,int}$ (μmol min^{-1} mg^{-1})
wild type	5.59[a] ± 0.046	41.4 ± 3.1
D253N	5.50[a] ± 0.056	35.3 ± 1.2
D273N	5.89[a] ± 0.023	2.02 ± 0.084
D275N	7.73[a] ± 0.16	0.131 ± 0.023
D279N	5.83[b] ± 0.052	0.223 ± 0.022

[a] The pK_{es} values for wild type, D253N, D273N, and D275N represent pK_a values. [b] The pK_{es} value for D279N represents a pK_b value.

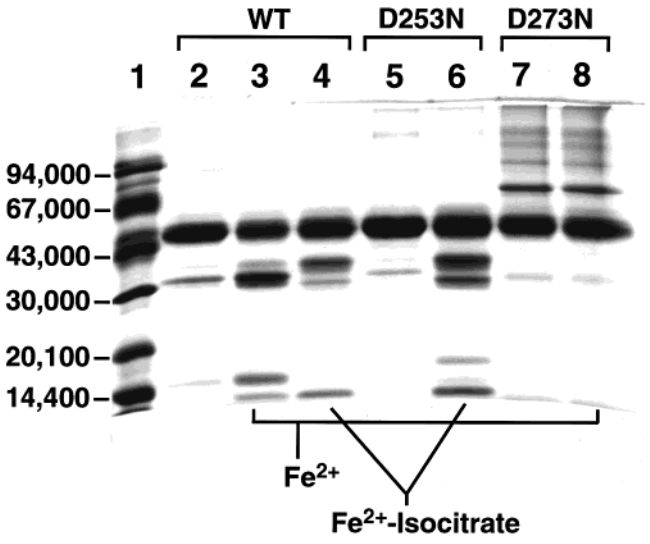

FIGURE 4: Fe^{2+}-affinity cleavage of porcine NADP-dependent isocitrate dehydrogenase. Wild type (lanes 2−4), D253N (lanes 5 and 6), and D273N (lanes 7 and 8) were incubated at 25 °C with ascorbate plus the following additions: none (lanes 2, 5, and 7); Fe^{2+} (lanes 3 and 8); or Fe^{2+} and isocitrate (lanes 4 and 6) as described under Experimental Procedures. Lane 1 contains protein standards.

value of V_{max} calculated by extrapolation of the double-reciprocal plot. The data of Figure 3C were analyzed by the equation:

$$V_{max,obs} - V_{max,lim} = (V_{max,int} - V_{max,lim})/(1 + [H^+]/K_a)$$

The data of Figure 3D were analyzed from the equation:

$$V_{max,obs} = V_{max,int}/(1 + K_b/[H^+])$$

which was analyzed by a double-reciprocal plot of $1/V_{max,obs}$ vs $1/[H^+]$. The pK_{es} and $V_{max,int}$ values are summarized in Table 3. In Figure 3, the points are the experimental data, while the lines represent fits to the above equations for $V_{max,obs}$ using the values of pK_{es} and $V_{max,int}$ given in Table 3.

Affinity Cleavage of Porcine NADP-Dependent Isocitrate Dehydrogenase by Fe^{2+} or Fe^{2+}-Isocitrate. Previous affinity cleavage studies of pig heart NADP-dependent isocitrate dehydrogenase (*10*), in the presence of Fe^{2+}-isocitrate, yielded two major pairs of peptides on inactivation: 30 + 17 kDa and 35 + 11 kDa, as compared with 46 kDa for the intact enzyme, as illustrated by the treatment of wild-type enzyme with Fe^{2+}-isocitrate in Figure 4 (lane 4). N-Terminal amino acid sequencing revealed that these peptides occur from mutually exclusive cleavages between Asp^{253}-Met^{254} or His^{309}-Gly^{310}, suggesting Asp^{253} and/or His^{309} as coordination sites for Fe^{2+}-isocitrate, and, by implication, Mn^{2+}-isocitrate. However, in the presence of Fe^{2+} alone, the predominant set of peptides, 32 + 15 kDa, was produced by a specific cleavage between Tyr^{272}-Asp^{273} upon inactivation, suggesting Asp^{273} as a coordination site for Fe^{2+} alone and, by implication, Mn^{2+}. This result is illustrated in Figure 4 (lane 3). Therefore, it was of interest to see whether the mutations at Asp^{253} and Asp^{273} eliminate the oxidative cleavages caused by Fe^{2+}-isocitrate and Fe^{2+}, respectively, in the presence of O_2. Fe^{2+}-isocitrate still inactivates D253N, and comparison of lanes 4 and 6 (Figure 4) shows that Fe^{2+}-isocitrate still cleaves and inactivates D253N in a manner similar to that of wild type. The results suggest that His^{309}, rather than Asp^{253}, is the important target for Fe^{2+}-isocitrate. Comparison of lanes 3 and 8 shows that the D273N mutation almost eliminates the oxidative cleavage and inactivation caused by Fe^{2+} in the wild-type enzyme. The results indicate that Asp^{273} is responsible for affinity cleavage by Fe^{2+} alone.

DISCUSSION

In this paper, site-directed mutagenesis has been used to evaluate the role of four aspartate residues in the catalytic reaction of porcine NADP-dependent isocitrate dehydrogenase. Asparagine was chosen to replace aspartate because asparagine lacks the negative charge, which is involved in binding metal cations, but retains a structure and size similar to aspartate. Characterization of the D253N, D273N, D275N, and D279N mutants suggests that the residues Asp^{273}, Asp^{275}, and Asp^{279} contribute to the enzyme's function, whereas Asp^{253} is not involved in enzyme function. Asp^{273} and Asp^{275} are important for the binding of divalent metal to porcine NADP-dependent isocitrate dehydrogenase, while Asp^{279} also plays a critical role in catalysis.

CD spectra and gel filtration FPLC were performed on all of the mutants to evaluate whether any of the mutations cause a disruption in the secondary structure of the enzyme or dissociation of the dimer. The results indicate that the mutations do not cause appreciable structural change in the enzyme.

The D275N mutant has greatly increased K_m values for Mn^{2+} and isocitrate compared to wild type, with a specific activity (as measured at pH 7.4) <0.1% that of wild type. The results suggest that Asp^{275} is important for binding catalytic metal to wild-type enzyme. Additionally, the D275N mutation causes a large increase in pK_a as compared to wild type. This increase in pK_a caused by changing Asp^{275} to a nonionizable group indicates that Asp^{275} has an important function in catalysis for this enzyme.

The D279N mutant has a specific activity that is <0.1% that of wild type, with only small increases in K_m for Mn^{2+} and isocitrate. However, the D279N mutation causes a major change in the shape of the pH−rate profile of the enzyme, with the V_{max} actually decreasing with increasing pH. This observation suggests that Asp^{279} may be a candidate for a catalytic base of the wild-type porcine NADP-dependent isocitrate dehydrogenase. The pH dependence of V_{max} observed in the D279N mutant probably reflects the ionization of another enzymatic amino acid normally masked by the larger effect of the ionization of Asp^{279} in the much more

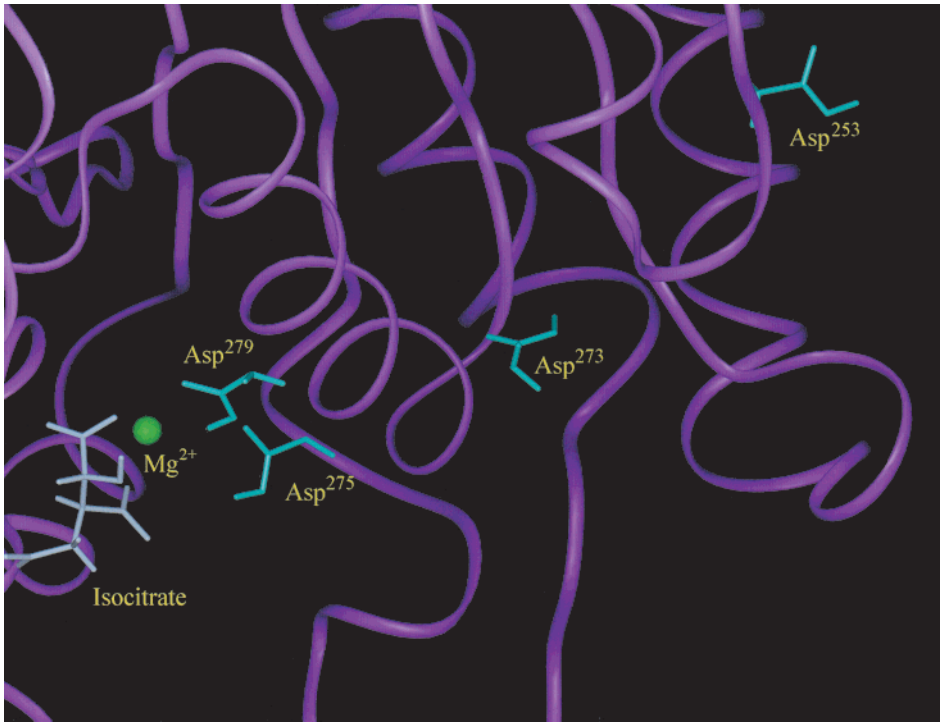

FIGURE 5: Homology model of the active site of porcine NADP-dependent isocitrate dehydrogenase. The four Asp residues mutated to Asn in this study are colored in cyan. The Mg ion is colored in green. Isocitrate is shown in white. This diagram was created using the Modeler program under Homology using Insight II as described under Experimental Procedures.

active wild-type enzyme; note the differences in $V_{max,obs}$ scales between Figures 3A and 3D.

In the reaction catalyzed by NADP-dependent isocitrate dehydrogenase, isocitrate is oxidized to oxalosuccinate by removal of a proton from the hydroxyl oxygen as well as of a hydride from the C2 position (*4*, *27*). A catalytic base would promote the removal of this proton. Previous studies (*14*, *15*) have shown that the p*K* of NADP-dependent isocitrate dehydrogenase represents ionization of a carboxyl group in the enzyme−substrate complex, which implies that a carboxylate group is involved in catalysis. ^{13}C NMR studies of isocitrate bound to isocitrate dehydrogenase showed that the carboxyls of isocitrate remain ionized over this pH range while the substrate is in the enzyme−isocitrate complex (*28*); these studies indicate that an enzymatic carboxylic acid residue, rather than isocitric acid, is responsible for the p*K* observed in the pH−V_{max} curves. This carboxylic acid residue is likely to be essential for catalysis.

Mutation of Asp^{273} to Asn also affected the kinetic characteristics of the enzyme. D273N exhibits a marked increase in the K_m for Mn^{2+} and a specific activity 5% that of wild type. Additionally, the D273N mutation eliminates the oxidative metal cleavage seen with Fe^{2+}alone in wild-type enzyme (*10*). These results indicate that Asp^{273} is important for binding metal ion, at least in the absence of isocitrate.

Previously, affinity cleavage of porcine NADP-dependent isocitrate dehydrogenase in the presence of O_2 + Fe^{2+}-isocitrate (*10*) had suggested that Asp^{253} and/or His^{309} are coordination sites for Fe^{2+}-isocitrate, and by implication Mn^{2+}-isocitrate. However, compared to wild type, mutation of Asp^{253} to Asn did not appreciably influence any of the enzyme's characteristics, including specific activity; pH−rate profile; K_m for Mn^{2+}, isocitrate, and NADP; and affinity cleavage. Therefore, it is likely that His^{309} is a coordination site for Mn^{2+} in the presence of isocitrate, whereas the cleavage produced between Asp^{253} and Met^{254}, which is relatively minor, is not the major cause of inactivation during affinity cleavage.

The only NADP-dependent isocitrate dehydrogenase whose structure has been solved is the *E. coli* enzyme with Mg^{2+}-isocitrate or NADP (*12*) bound to it. Although there is only about 14% identity between the amino acid sequences of the mammalian (porcine) and bacterial (*E. coli*) enzymes, sequence alignment of these and other known isocitrate dehydrogenases using CLUSTAL W shows that many of the residues involved in the metal-isocitrate site are conserved (*3*). Figure 1 shows that Asp^{253} can be aligned with Asp^{279} of the *E. coli* enzyme, which is close in the sequence to Asp^{283}. $Asp^{283'}$ (from the second subunit) is liganded to Mg^{2+} in the *E. coli* structure (*12*). However, in the pig heart enzyme, Asp^{253} does not seem to have a comparable function, since the D253N mutant is similar to wild-type enzyme in its kinetic properties. The porcine enzyme's Asp^{275} can be aligned with Asp^{307} of the *E. coli* enzyme, which is liganded to the Mg^{2+} ion (*12*), whereas Asp^{279} in the porcine enzyme corresponds to Asp^{311} in *E. coli*, which is also near the Mg^{2+} ion (*12*). The porcine enzyme's Asp^{273}, which was oxidatively cleaved by Fe^{2+} in the absence of isocitrate (*10*), is conserved in the eukaryotic NADP-dependent isocitrate dehydrogenases, but not in *E. coli*. Asp^{273} is near Asp^{275}, which was already mentioned to be aligned with Asp^{307} of the *E. coli* enzyme.

Using the Modeler program of Insight II, a structure for porcine NADP-dependent isocitrate dehydrogenase was constructed to allow visualization of the metal-isocitrate site (Figure 5). This model was based on the X-ray coordinates of the *E. coli* enzyme (*12*) and the alignment of the amino

acid sequences of the mammalian enzymes with *E. coli* enzyme. Figure 5 shows that a carboxyl oxygen of Asp^{253} is approximately 25 Å from the Mg^{2+}, which is consistent with the result that Asp^{253} is not involved in the coordination of divalent metal to the porcine enzyme in the presence of bound isocitrate. A carboxyl oxygen of Asp^{273}, which was found to be a site of oxidative cleavage in the absence of isocitrate (*10*), is about 13 Å from the bound Mg^{2+}. However, this structure is modeled in the presence of bound isocitrate; in the absence of bound isocitrate, this residue might move closer to the bound divalent metal ion. The carboxyl oxygens of both Asp^{275} and Asp^{279} are close to bound metal in the modeled structure: approximately 3.5 and 3.6 Å, respectively. This distance is consistent with the result that substitution of Asp^{275} by Asn caused a large increase in the K_m for Mn^{2+}. Earlier ^{113}Cd NMR studies (*29*) indicated that the porcine enzyme−metal-isocitrate complex is coordinated to six oxygen ligands, or one nitrogen and five oxygen ligands (*10*). Thus, several Asp residues are most likely coordinated to the bound metal in NADP-dependent isocitrate dehydrogenase.

A carboxyl oxygen of Asp^{275} is about 5 Å from a carboxyl oxygen of Asp^{279} in the porcine enzyme. Mutation of each of these residues to Asn resulted in major changes in their respective pH−rate profiles, suggesting that one of these residues is the catalytic base. Even though these residues are about 4.0−4.5 Å from the hydroxyl of isocitrate, one of them (perhaps Asp^{279}) can still act as a general base if a water molecule is positioned between the Asp residue and isocitrate: the Asp residue can activate water, which in turn can remove a proton from the hydroxyl oxygen of isocitrate to yield the negatively charged alkoxide ion. The carbon-linked hydrogen of an alkoxide ion should be easily removed as a hydride ion (*30*), resulting in the transfer of hydrogen to NADP and the formation of oxalosuccinate. It is possible that water might be bound to the metal ion and to Asp (*28*). It has previously been shown that the reaction is slower in D_2O than in H_2O, indicating that proton transfer is a determinant of the rate of the reaction (*31*).

The reaction catalyzed by NADP-dependent isocitrate dehydrogenase occurs in two steps: isocitrate is first oxidized to oxalosuccinate (*27*), and the β-carboxylate of oxalosuccinate is then lost as CO_2 to form α-ketoglutarate (*32*). The metal ion appears to have two functions in these reactions. The divalent metal is required for binding of the substrate isocitrate to the enzyme (*33*), and helps stabilize the negative charge of the enolate intermediate formed during the decarboxylation step (*34*). This could require two binding sites for the divalent metal to the enzyme: one in the absence of isocitrate, the other in the presence of isocitrate. However, only one metal binding site per subunit has been found in the absence or presence of isocitrate (*4*). These sites may be different, but are mutually exclusive. This explanation would be consistent with a role for Asp^{273} as a coordination site for Mn^{2+} in the absence of isocitrate, whereas Asp^{275} and perhaps His^{309} are coordination sites for Mn^{2+} in the presence of isocitrate. Prior to the availability of a crystal structure of the mammalian NADP-dependent isocitrate dehydrogenase, the homology model is useful to summarize and conceptualize the experimental results.

ACKNOWLEDGMENT

We thank Dr. Yu-Chu Huang for performing N-terminal amino acid sequencing and for her help in preparing some of the mutants. We also thank Christine McDaniel for performing nucleotide sequencing.

REFERENCES

1. Kelly, J. H., and Plaut, G. W. E. (1981) *J. Biol. Chem. 256*, 330−334.
2. Bailey, J. M., and Colman, R. F. (1985) *Biochemistry 24*, 5367−5377.
3. Haselbeck, R. J., Colman, R. F., and McAlister-Henn, L. (1992) *Biochemistry 31*, 6219−6223.
4. Colman, R. F. (1983) *Pept. Protein Rev. 1*, 41−69.
5. Villafranca, J. J., and Colman, R. F. (1972) *J. Biol. Chem. 247*, 209−214.
6. Colman, R. F. (1972) *J. Biol. Chem. 247*, 215−223.
7. Bailey, J. M., and Colman, R. F. (1987) *Biochemistry 26*, 4893−4900.
8. Northrop, D. B., and Cleland, W. W. (1970) *Proc. Fed. Am. Soc. Exp. Biol. 49*, 408.
9. Ehrlich, R. S., and Colman, R. F. (1976) *Biochemistry 15*, 4034−4041.
10. Soundar, S., and Colman, R. F. (1993) *J. Biol. Chem. 268*, 5264−5271.
11. Hurley, J. H., Thorsness, P. E., Ramalingam, V., Helmers, N. H., Koshland, D. E., and Stroud, R. M. (1989) *Proc. Natl. Acad. Sci. U.S.A. 86*, 8635−8639.
12. Hurley, J. H., Dean, A. M., Koshland, D. E., and Stroud, R. M. (1991) *Biochemistry 30*, 8671−8678.
13. Stoddard, B. L., Dean, A., and Koshland, D. E. (1993) *Biochemistry 32*, 9310−9316.
14. Colman, R. F. (1973) *J. Biol. Chem. 248*, 8137−8143.
15. Colman, R. F. (1968) *J. Biol. Chem. 243*, 2454−2464.
16. Michaelis, L., and Mizutani, M. (1925) *Z. Phys. Chem. (Leipzig) 116*, 135.
17. Mizutani, M. (1935) *Z. Phys. Chem. (Leipzig) 118*, 318.
18. Mizutani, M. (1925) *Z. Phys. Chem. (Leipzig) 116*, 350.
19. Grodsky, N. B., Soundar, S., and Colman, R. F. (1999) *FASEB J. 13*, A1444.
20. Soundar, S., Jennings, G. T., McAlister-Henn, L., and Colman, R. F. (1996) *Protein Expression Purif. 8*, 305−312.
21. Tao, B. Y., and Lee, K. C. P. (1994) in *PCR Technology: Current Innovations* (Griffrin, H. G., and Griffin, A. M., Eds.) p 74, CRC Press, Cleveland, OH.
22. Sarkar, G., and Sommer, S. S. (1990) *BioTechniques 8*, 404.
23. Laemmli, U. K. (1970) *Nature 227*, 680−685.
24. Johanson, R. A., and Colman, R. F. (1981) *Arch. Biochem. Biophys. 207*, 9−20.
25. Greenfield, N., and Fasman, G. D. (1969) *Biochemistry 8*, 4108−4116.
26. Mas, M. T., and Colman, R. F. (1985) *Biochemistry 24*, 1634−1646.
27. Siebert, G., Carsiotis, M., and Plaut, G. W. E. (1957) *J. Biol. Chem. 226*, 977−991.
28. Ehrlich, R. S., and Colman, R. F. (1987) *Biochemistry 26*, 3461−3466.
29. Ehrlich, R. S., and Colman, R. F. (1989) *Biochemistry 28*, 2058−2065.
30. Jencks, W. P. (1969) in *Catalysis in Chemistry and Enzymology*, pp 152−153, McGraw-Hill, New York.
31. Colman, R. F., and Chu, R. (1969) *Biochem. Biophys. Res. Commun. 34*, 528−535.
32. Londesborough, J. C., and Dalziel, K. (1968) *Biochem. J. 110*, 223−230.
33. Levy, R. S., and Villafranca, J. J. (1977) *Biochemistry 16*, 3293−3301.
34. Steinberger, R., and Westheimer, F. H. (1951) *J. Am. Chem. Soc. 73*, 429−435.

BI9919753